DISCLAIMER

This report was prepared as an account of work sponsored by an agency of the United States Government. Neither the United States Government nor any agency thereof, nor any of their employees, makes any warranty, express or implied, or assumes any legal liability or responsibility for the accuracy, completeness, or usefulness of any information, apparatus, product, or process disclosed, or represents that its use would not infringe privately owned rights. Reference herein to any specific commercial product, process, or service by trade name, trademark, manufacturer, or otherwise does not necessarily constitute or imply its endorsement, recommendation, or favoring by the United States Government or any agency thereof. The views and opinions of authors expressed herein do not necessarily state or reflect those of the United States Government or any agency thereof. Reference herein to any social initiative (including but not limited to Diversity, Equity, and Inclusion (DEI); Community Benefits Plans (CBP); Justice 40; etc.) is made by the Author independent of any current requirement by the United States Government and does not constitute or imply endorsement, recommendation, or support by the United States Government or any agency thereof.

LA-UR-25-31601

Approved for public release; distribution is unlimited.

Title:	Modeling and Design of a Sub-Nyquist PDV Digitization System
Author(s):	Mills, Gabriel Thomas
Intended for:	Report for Master of Engineering degree credit Report
Issued:	2025-11-25

Modeling and Design of a Sub-Nyquist PDV Digitization System

Gabe Mills
Intelligence and Space Research,
Los Alamos National Laboratory
Los Alamos, New Mexico, USA
gmills@lanl.gov

***Abstract*—Photon-Doppler Velocimetry (PDV) uses interferometry of a transmitted optical signal reflected from a fast-moving device under test (DUT) to generate a product signal at a doppler-shifted frequency which is proportional to the velocity of the object being measured. The technique has applications in shock physics, where it is used to measure fast-moving objects over a short lifespan of travel, such as a bullet, shrapnel, or other shock-accelerated object. In many cases, this doppler-shifted optical signal reflected from the object is detected and transformed into an electrical radio-frequency (RF) signal by an opto-electrical device known as a photodetector. In typical lab bench tests, this RF signal representing the doppler velocity shift is captured and digitized by an expensive, high sample rate oscilloscope or similar tool, as the Nyquist frequency is extremely high and the doppler-shifted RF signal can swing up to several GHz. The purpose of this investigation is to evaluate the feasibility and design of a low Size, Weight, and Power (SWaP) digitizer and RF downconversion system to replace the aforementioned digitization bench tools. This design aims to utilize sub-Nyquist sampling and reconstruction techniques to reconstruct the full-band signal from a downconverted and decimated time-series acquisition, as most small, low-SWaP digitizer products on the market have sample rates significantly below the expected maximum doppler frequency. Computer modeling techniques can also be used to probe and predict the effectiveness of this design and are discussed in turn.**

***Index Terms*—Photon-Doppler Velocimetry, frequency conversion, Nyquist-Shannon sampling theorem, digitization, undersampling**

I. Introduction

A. Background

In the simplest case, a Photon-Doppler Velocimetry (PDV) measurement system uses an optical interferometric doppler-shifted signal created from a source laser being reflected off the device under test (DUT). The system contains a laser which is fed through an optical circulator or coupler, through a fiber cable to the probe where the emitted light is reflected off of the DUT and reenters the cable via the probe, illustrated in Figure 1. The reflected optical signal then travels back down the cable, through the coupler, and out the next adjacent port, where it is recombined with the source laser (often split or coupled off of the source emission) in an optical detector, where they interfere and output the difference, or beat, frequency between the doppler shifted signal and the source. This beat frequency

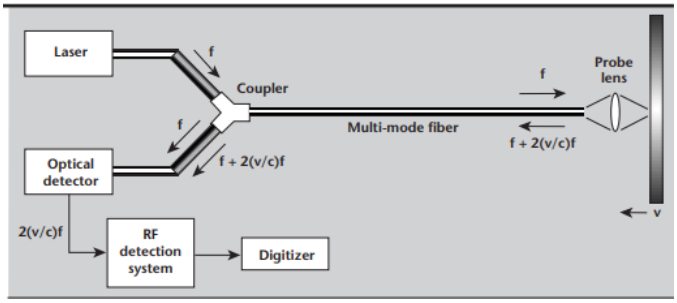

Fig. 1. General PDV block diagram [1].

B is directly related to the velocity of the DUT v and the wavelength of the optical laser λ [1, 2].

$$B = \frac{2}{\lambda}|v| \tag{1}$$

In theory, this resultant optical signal is the pure doppler shift frequency due to the velocity of the DUT.

PDV experiments using a "flyer-plate" device will be the focus of attention for this design and investigation. This configuration uses an explosive charge to propel a metal plate, which presents a consistent reflective surface for the PDV probe and presents a consolidated object to impart the doppler shift onto the interferometer [1, 2].

For this application, the resulting PDV time-series data is typically analyzed via the creation of a spectrogram plot. In simple terms, the signal at the input to the oscilloscope or digitizer can be considered as a narrowband single tone that sweeps across some wide frequency band proportional to the velocity of the DUT. The raw time-domain data is sliced into bins or "frames" along the time axis, and a Fast Fourier Transform (FFT) is applied to each frame [2]. This is relatively trivial to do in a computer programming environment such as MATLAB or Python. The resulting frequency versus time plot shows the doppler shift over time. The conversion from doppler space to velocity space is direct, and thus a velocity versus time plot can be extracted merely by adjusting the scale of the vertical axis. Example velocity plots extracted from a PDV spectrogram are shown in Figure 2.

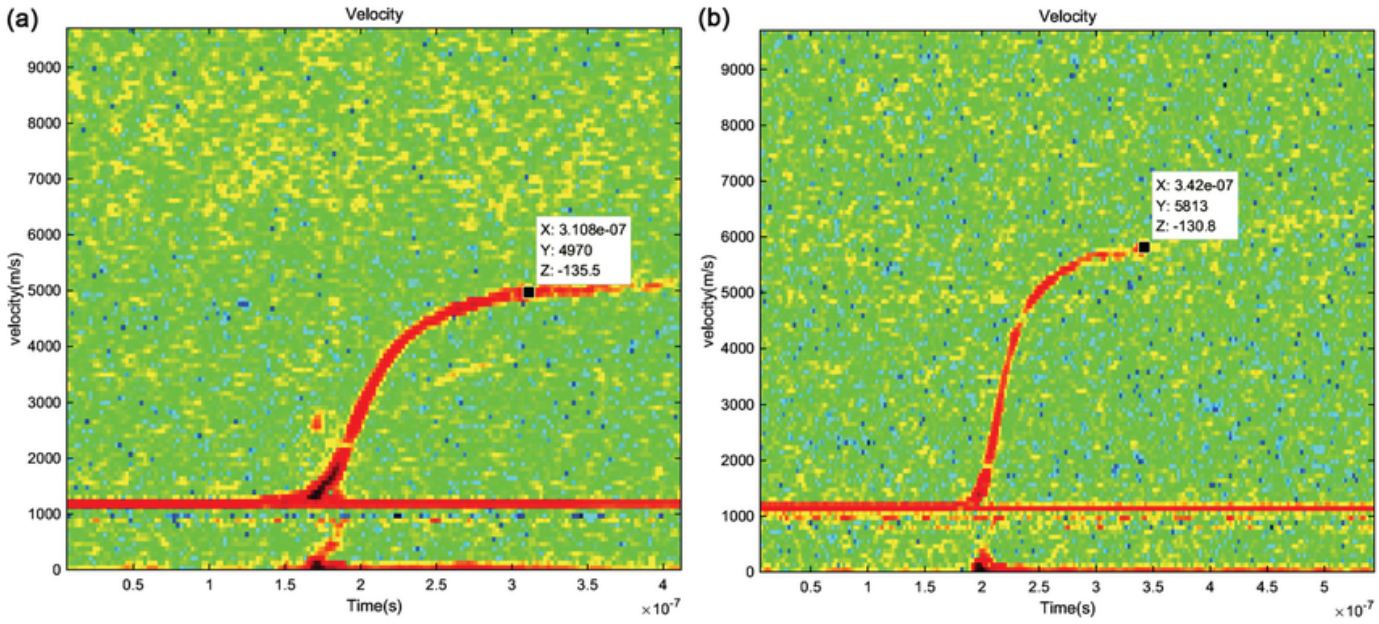

Fig. 2. Example flyer plate PDV spectrograms. Note the velocity curves begin around 1000 m/s, with the jump from 0 to 1000 m/s not visible, likely due to the instantaneous acceleration of the DUT. The curve roughly follows a sigmoid S-shape, with the velocity leveling off near the end of travel [3].

B. PDV Spectrograms

As can be seen in the example plot in Fig. 1, PDV flyer-plate spectrograms take a common "parent" form. At the beginning of the travel of the DUT there is a sharp, sometimes invisible "rising edge" in the signal as the flyer plate starts to move. Even with high sample rates this segment of the chart is difficult to observe using an FFT spectrogram, as with the nature of the devices typically tested (often explosives) the initial acceleration is too rapid and may occur within the span of one FFT sample bin. This "rising edge" can be seen in the above example at around 0.15 microseconds. Note that the trace appears around 1000 km/s and the "jump-off" from 0 km/s to 1000 km/s is not visible [3].

After the jump-off, the instantaneous velocity of the flyer or DUT becomes slow enough to plot across the rest of its travel. This is the utility of the spectrogram; it usually is unable to see the exact timing and behavior of the near-instantaneous acceleration event, but it will catch the velocity characteristics of the DUT throughout the rest of its travel. Also notable in the spectrogram is the presence of a single-tone artifact, which can be a result of the architecture of the PDV optical system (for example, the local oscillator from a heterodyne conversion bleeding through) [2].

C. PDV Sampling

Conventionally, as the Nyquist and Shannon criteria states, to get a clear measurement of the doppler velocity without aliasing, the oscilloscope digitizing the PDV signal would need to sample at a rate at least double the maximum frequency seen at its input [11]. In practice it proves useful to sample at multiple times the Nyquist rate to obtain accurate phase information, and to provide enough time-domain samples to allow the analyst ample time resolution in the spectrogram plot (since it is computed by creating FFT slices from bins of time-domain samples). Therefore, in conventional PDV analysis, high-sample-rate digitizers and oscilloscopes are the norm. Because this equipment is readily available in the typical laboratory setting, analysis of the minimum feasible hardware for acquisition of useful PDV data has not yet been performed.

D. Overview

This investigation aims to analyze the requirements and application of a low-SWaP digitization and radio-frequency (RF) down-conversion system for PDV measurements, for cases where standard optical and RF digitization equipment is not feasible due to SWaP constraints. The investigation will contain multiple facets including: analyzing the effect aliasing has on the signal due to a low, sub-Nyquist digitization sample rate, design considerations and possible implementations of an RF down-conversion system to divide the wideband signal to fit into a low-bandwidth digitizer input, and exploring possible avenues for signal reconstruction and modeling after successful deployment of the system.

II. Concepts

A. Undersampling

As briefly discussed above, time-series digitization of RF signals conventionally adheres to the theorem set forth by Shannon and Nyquist [11], which states that the frequency content of any signal can be completely reconstructed provided that it was sampled at a rate greater than or equal to twice its highest frequency component (this frequency being referred to as the Nyquist frequency). Additionally, it can prove beneficial

to sample at multiples of this frequency to preserve phase information, as the Nyquist limit only guarantees that frequency content is recovered, and higher fidelity is needed to acquire additional data. In this investigation, however, the case is considered where, due to general hardware limitations, a given signal is only able to be sampled at a fraction of its Nyquist frequency. With no other signal manipulation the result of this sub-Nyquist undersampling is fairly straightforward to investigate as it relates to a typical PDV measurement, as existing time-series data can be simply decimated by a factor equivalent to the ratio between the original and undersampled rates.

B. Aliasing and Folding

To build an understanding of how sub-Nyquist digitization might affect the signal of interest, the general effect of aliasing on undersampled data must first be investigated. The notion of aliasing describes signal behavior observed when a low-frequency "version" or *alias* of high-frequency content is created when an input signal is sampled at a rate below its Nyquist frequency [4]. In classroom and textbook cases, this is understood to be a negative outcome in a signal processing system, as the signal aliases can overlap or obscure the desired signal. Since the aliased high frequency data appears as a low-frequency copy of the real high-frequency content, there is no way to distinguish the aliasing from the intended low-frequency content. In the case where aliasing is a concern in a given digitization system, and a higher sample rate is not an option, the conventional approach to preventing aliasing is to implement a bandpass or lowpass filter prior to sampling. This attenuates high frequency content that would otherwise present itself on top of the low frequency content, and thus prevents any additional content from accumulating on the intended measurement band.

An additional pattern that is of note to this investigation is the notion that aliasing content will appear to "fold" over the Nyquist frequency of the digitization system [5]. That is, high-frequency aliasing content will appear in the low-frequency band at a location equidistant from the Nyquist frequency as the original high-frequency content, as shown in Figure 4. For example, a signal with single-tone content at 1.5 GHz sampled at 1 GHz will see an aliased copy of the 1.5 GHz tone at 500 MHz. An important element of this behavior that is prudent to consider in the design of this project is that without additional context, the ability to discern what the original frequency was is lost.

The concepts of aliasing and folding, although simple, are fundamental to the understanding and characterizing the output behavior of a sub-Nyquist sampled signal. Combining these concepts with the general form of a PDV experiment signal, the (typically unwanted) characteristics of an undersampled signal can be taken advantage of and used to benefit the design of a low SWaP digitizer system.

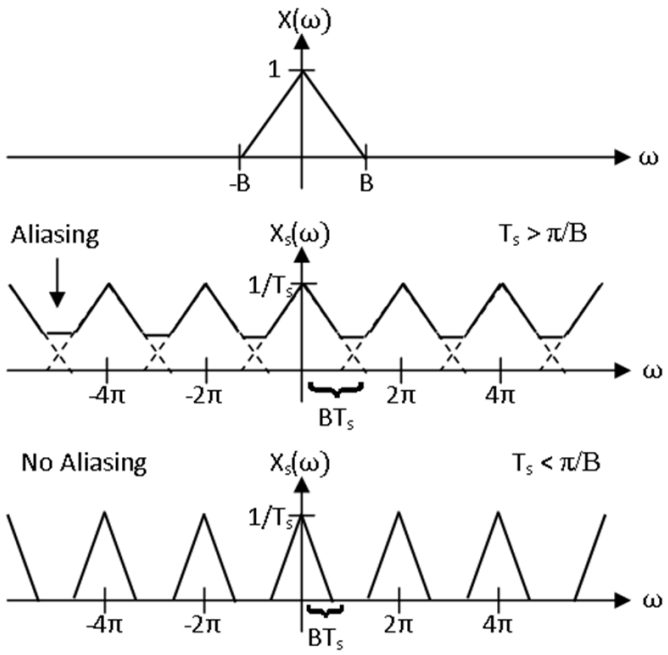

Fig. 3. Aliasing diagram [4]. In the aliasing plot, the lower edges of the higher-frequency triangles alias and merge into the range of the lower ones, an often-undesired effect.

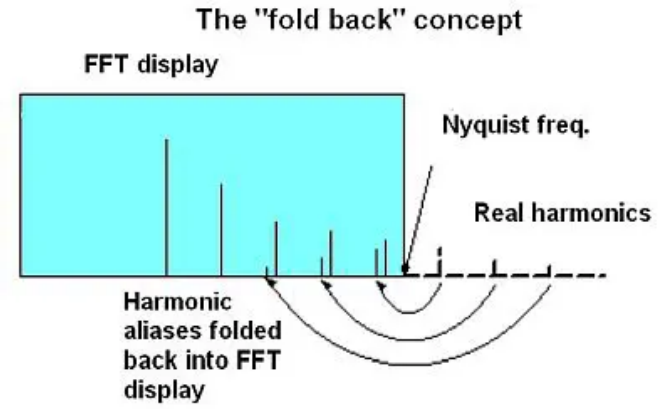

Fig. 4. Folding of aliased frequencies [5]. The lower-frequency alias of each high frequency spike shows up at a location equidistant from the edge of the blue rectangle, as if they had "folded over."

C. RF Conversion

The utilization of aliasing to view the entire folded signal can be compounded if the use of RF conversion techniques to manipulate the input bandwidth is considered. Aliasing solves part of the problem already, but as is described in later sections of this paper, the intended sample rate is a small fraction of the full Nyquist frequency of the input signal. Due to this large discrepancy, merely analyzing the aliasing behavior is insufficient, as the input PDV signal may shift in frequency too fast for much of the signal to be decipherable. Thus, it becomes necessary to add some amount of conditioning to the signal prior to sampling and

digitization to mitigate this issue.

Consider a PDV signal that shifts between 0 and 3 GHz in the span of 100 microseconds, and a digitizer that samples on the order of 100 megasamples per second (MSPS). The digitizer's Nyquist frequency then becomes half the sample rate, 50 MHz, which misses the signal's Nyquist frequency by a factor of 60. It follows that the signal will then "fold" into the 50 MHz digitizer band 60 times in the span of 100 microseconds. This amount of rapid folding in the aliased signal makes analysis difficult, as tracking the number of folds in the spectrogram to extract the original frequency becomes more complicated. Additionally, in this application, the initial "jump-off" observed in PDV data as described in the introductory section of this paper further obfuscates the original frequency shift as the initial acceleration and jump in frequency is too fast to be resolved in a spectrogram and is lost.

To address this problem, a combination of a few basic RF components can be used to divide the signal into segments based on frequency, and shift each segment into the input range of the digitizer. The primary processing technique that can be applied is frequency down-conversion, where the input signal is mixed with a local oscillator (LO) to create an output signal at sum and differences of the input frequency and LO frequency.

An ideal mixer with local oscillator frequency f_{LO} and input frequency f_{RF} creates output products at $f_{up} = f_{RF}+_{LO}$ and $f_{dn} = f_{RF} - f_{LO}$. Realistic realizations of RF mixers are often band limited and cannot always support both conversion products on the output, but in some cases, both can be observed and used.

Initially, only down-conversion will be investigated, where the difference output is the desired product of the mixing step. If RF power dividers are added prior to the mixing step, a PDV input signal can be divided evenly into frequency segments or "channels," each to be mixed with a separate LO to drop each frequency channel into the same frequency range. Low-pass or band-pass filtering can be used after this step to prevent unwanted mixer products from interfering with the converted signal.

For an example, the same PDV input signal moving from 0 – 3 GHz can be split into a set of twelve 0-250 MHz "channels," each with their own LO. That is, the first channel captures the input signal from 0-250 MHz which needs no down-conversion, the second channel captures the input from 250 - 500 MHz which is mixed down with an LO frequency of 250 MHz, the third channel captures 500 – 750 MHz which is mixed with 500 MHz, and so on. Each channel can be low-pass filtered to limit the input band such that it only contains the desired "slice" of frequency content. Now, a 100 MSPS digitizer looking at one of these channels only has to contend with fitting a 250 MHz signal segment into a 50 MHz Nyquist zone, which folds a mere 5 times. More importantly, the signal can be tracked from channel to channel, and the mere appearance of the signal on one of these channels reintroduces partial knowledge of the original frequency, even though it is not present in the spectrogram. For instance, returning to the example, a sampled signal appearing on "channel 4" (1000 – 1250 MHz downconverted with a 1 GHz LO) at 150 microseconds means that the input signal must have crossed into the 1000 – 1250 MHz range at that time.

D. Negative Frequencies

As detailed in previous sections, the input signal in question can be considered to be a band-limited, continuous-wave, single-tone periodic signal that increases in frequency over time. Thus, the signal is purely real and must contain a negative image of its positive frequency content. Illustrating this: Consider the instantaneous PDV output as a sinusoidal signal

$$f(t) = cos(\omega_0 t) \tag{2}$$

where ω is the instantaneous doppler shift frequency. To view the content of this signal in the continuous frequency domain, a Fourier transform must be applied:

$$F(\omega) = \int_{-\infty}^{\infty} cos(\omega_0 t) * e^{-j\omega t} dt \tag{3}$$

$f(t) = cos(\omega_0 * t)$ can also be represented as

$$f(t) = \frac{1}{2}[e^{j\omega_0 t} + e^{-j\omega_0 t}] \tag{4}$$

Using Euler's formula it can be equated back to $f(t)$:

$$\begin{gathered} f(t) = \frac{1}{2}[e^{j\omega_0 t} + e^{-j\omega_0 t}] = \\ \frac{1}{2}[cos(\omega_0 t) + jsin(\omega_0 t) + cos(\omega_0 t) - jsin(\omega_0 t)] \\ = cos(\omega_0 t) \end{gathered} \tag{5}$$

Inserting this exponential decomposition into the Fourier integral,

$$F(\omega) = \frac{1}{2}\int_{-\infty}^{\infty} [e^{j\omega_0 t} + e^{-j\omega_0 t}] * e^{-j\omega t} dt \tag{6}$$

Which can be separated into two integrals

$$F(\omega) = \frac{1}{2}\left[\int_{-\infty}^{\infty} e^{j\omega_0 t} * e^{-j\omega t} dt + \int_{-\infty}^{\infty} e^{-j\omega_0 t} * e^{-j\omega t} dt\right] \tag{7}$$

And using the Fourier pair

$$G(\omega) = \int_{-\infty}^{\infty} e^{j\omega_0 t} * e^{-j\omega t} dt = 2\pi\delta(\omega - \omega_0) \tag{8}$$

The Fourier representation of the input signal f(t) becomes

$$F(\omega) = \pi(\delta(\omega - \omega_0) + \delta(\omega + \omega_0)) \tag{9}$$

which shows that for an arbitrary input frequency ω_0, spectral content exists at ω_0 and $-\omega_0$, and is represented as impulses for the case where the input frequency is a single-tone sinusoid.

Because of the negative frequency signal image, the frequency conversion design under consideration can be massively simplified if the "extra" content is accounted for. Negative frequency content can be manipulated in the same manner as positive signal content when using RF conversion and mixing; thus with clever selection of local oscillators negative frequencies can be upshifted into the range of the digitizer and positive, higher frequency content can be shifted down into the same range.

If the additional conversion products are added into the mixing step, the number of channel divisions can be cut in half. When accounting for both the positive and the negative content, the sum and difference products can now be used; as for one local oscillator, a positive segment of the signal frequency band is downshifted (difference), and another negative segment is upshifted (sum) into the target input band, crossing 0 Hz (DC). Again, using the above example with a digitizer input of 0-250 MHz, a local oscillator of 250MHz can be used to down-convert the input signal content from 250 – 500 MHz to 0 – 250 MHz as well as upshift the content from 0 to -250 MHz into the same band. Therefore, 500 MHz of the example signal can be shifted into the 250 MHz input band using a single 250 MHz local oscillator, which is double the content accounted for in the original.

III. Modeling

A. Mock Input Signal

A simple model can now be created to evaluate the general behavior of an undersampled PDV flyer-plate signal. For this discussion, the conversions to velocity in the output spectrograms are omitted for clarity, since the investigation primarily focuses on frequency conversion. Python was used as the programming environment, using NumPy and MatPlotLib for computation and display. First, a faux PDV output signal needs to be created to form the input to the model. When looking at the example PDV data spectrograms shown in the introductory section, it can be noted that the frequency shift signal, negating ringing and undesired artifacts, very roughly resembles a logarithm or sigmoid function in appearance. Hence, for this basic model, the raw PDV input signal can be substituted for a "boiler-plate" function, in this case an arbitrary sigmoid.

To create the RF input signal, the PDV doppler frequency shift function must then be used to modulate a cosine function. This signal represents the original RF input incident on the downconversion hardware, and the result of the optical interferometry. This is as simple as defining a signal vector as the result of the cosine of the sigmoid function vector multiplied by a time vector, which is incremented by the desired sample period, with a length equal to the expected experiment duration. The "jump-off" can be simulated by zeroing the function for a set wait time (in this case, 50 microseconds) to create an instantaneous jump to the sigmoid curve, roughly approximating the behavior of the DUT experiencing near-instantaneous acceleration. The resulting boiler-plate PDV signal is shown in Figure 5. Some of the modeling parameters can be arbitrary, and for now the sample period and frequency will be set to 40 picoseconds and 25 GHz respectively to mimic the sample rate of a high-end digitizer. Similarly, the experiment duration is set to 200 microseconds. Moving away from the previously discussed example, the digitizer sample rate will now be set to 200 MSPS for this model, and the maximum doppler shift will be set to 3 GHz.

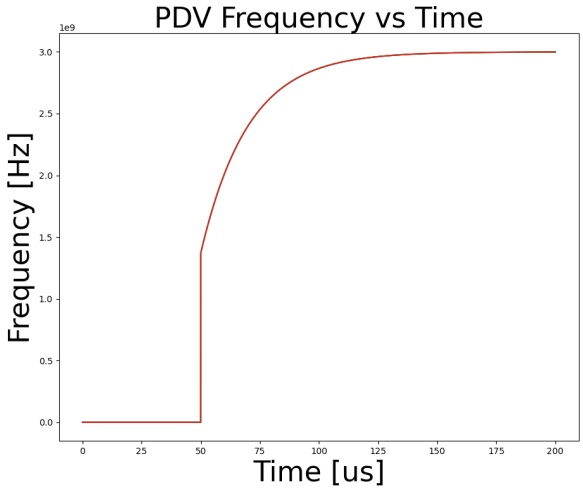

Fig. 5. Boiler plate PDV signal. Note the "jump-off" (instantaneous rise time) between 0 and approximately 1.5 GHz.

B. Raw Undersampling

As a point of comparison to show what the aliasing behavior looks like without any downconversion, the RF input can first be crudely decimated by a factor equal to the ratio between the input sample rate and the anticipated undersampling rate. No extra processing needs to be added here. It is, however, important to be careful at this step, because built-in decimating functions such as those found in MATLAB libraries include low-pass anti-alias filters, which in this specific case are not helpful. Once the signal is decimated, it can be sliced into FFT spectrums to create a spectrogram.

To create the spectrogram, a simple algorithm can be constructed. The window and shift sizes must be first selected, which define the number of time-domain samples of the signal per FFT slice and the overlap between each slice,

respectively. The algorithm consists of a loop that divides the signal length into these windows, and computes the FFT of each window. The resulting FFT frame slices are added into an output array, which can be easily plotted using the MatPlotLib imshow() or MATLAB's waterfall() function. The window and shift values are set to even powers of 2. The result of this plot is shown in Figure 6.

The aliasing and folding behavior can be seen on full display in the output spectrogram. The maximum frequency plotted is 100 MHz, the Nyquist frequency for the undersampled rate. For the signal in question, a single tone sweeping over 0 to 3 GHz, the signal should fold back on itself 15 times (equal to the ratio of the maximum frequency to the sampling frequency). Here, as expected, the first few folds that occur as the signal begins to move (around 40 microseconds) are not able to be resolved, as these correspond to the instantaneous jump-off (seen along the vertical axis of the doppler signal plot between 0 and approximately 1.4 GHz). Only 12 folds can be accounted for. Compounding this issue, the early segments of the undersampled signal are of noticeably lower brightness and resolution due to the more rapidly shifting signal frequency during this time period. In this sterile modeling environment they are still discernible, but this will likely not be the case for a real experiment with varying power levels, additive noise, loss, dispersion, etc.

C. Undersampling with Downconversion

Now that the raw undersampled signal has been computed and displayed, adding some fidelity to the model to represent the frequency division is fairly straightforward. The first step is to add a downshifting and division step. This models the mathematical role of the RF mixers on each channel, and is most easily done by multiplying the incoming mock PDV signal with individual cosine terms in the time domain. For this example, with a digitizer Nyquist rate of 100 MHz, each channel will be set to a bandwidth of 300 MHz, dividing the full signal into 5 channels. It is expected that content appears across all 5 channels at different times, and "fold" into the Nyquist band of the digitizer 3 times. As discussed in the Negative Frequencies section, the local oscillators will be placed in the center of each band to maximize bandwidth, resulting in LO frequencies of 300, 900, 1500, 2100, and 2700 MHz. Each downconverted channel is then low-pass filtered at 300 MHz to represent an equal input bandwidth limit on the digitizer.

Similar to the creation of the previous plots, new spectrograms with sliding windows are created, this time for all 10 frequency division channels. Note the lack of frequency content on many of the plots due to the initial rapid increase in doppler frequency. This new series of spectrograms is shown in Figure 7. As expected, the signal is visible for the longest time period on the last channel, once the acceleration has decreased. Now that the theory of operation of the system has been evaluated and analyzed, the concepts can be applied to a realistic design that can be implemented into hardware.

IV. Preliminary Design and Benchtop Model

With the high-level discussion and examples complete, a preliminary proof-of-concept design for the RF front end can now be built from new, realistic signal requirements. The real PDV signal intended for measurement in this project was expected to reach a peak frequency shift less than or equal to 4 GHz. The design will focus on cheap, available connectorized components suitable for benchtop testing, and may not fully represent a finalized, refined implementation. Components were sourced from retailers such as Mini-Circuits or Digikey, and again availability and cost were the key driving factors for these components.

A. Digitizer Selection

As with the RF components, the digitizer selected must be available, low-cost, and additionally, as set forth in the introduction to this project, low SWaP. The digitizer chosen must also be relatively straightforward to set up for measurement and fast to implement with little reliance on external hardware. The most important internal specifications to consider for selecting a digitizer model are RF input bandwidth and sample rate. Referencing the earlier background discussion, the importance of the sample rate should be obvious, as it determines the Nyquist frequency and thus the folding and aliasing behavior of the undersampled signal.

One family of solutions that fits all the listed criteria for selection is the Red Pitaya line of single-board computers (SBCs), designed by a company out of Slovenia sharing the same name [6]. These SBCs contain a set of 4 SMA RF inputs and outputs, an onboard programmable field-programmable grid array chip FPGA for signal processing, and a host of general-purpose input and output (GPIO) ports. The boards can be easily programmed and controlled remotely as well. Several variants are currently available with different target applications and use cases. Most models currently on the market sample the RF ports at or around 125 MSPS with an RF front end designed around the digitizer Nyquist frequency at 60 MHz [6]. However, one particular variant fits the design criteria rather well: the Red Pitaya SDR122-16, which supports a sample rate of 122 MSPS, but uses different RF front end components to widen the input bandwidth. The listed bandwidth supported is 300 kHz to 550 MHz [6].

The SDR122-16 is particularly useful to this design as it is designed specifically to support undersampling, which is the exact use case in question [6]. This model costs about $720 and is regularly stocked from mainstream vendors such as Digikey, meeting the need for being low cost, readily available, and easy to acquire. They are small, meaning

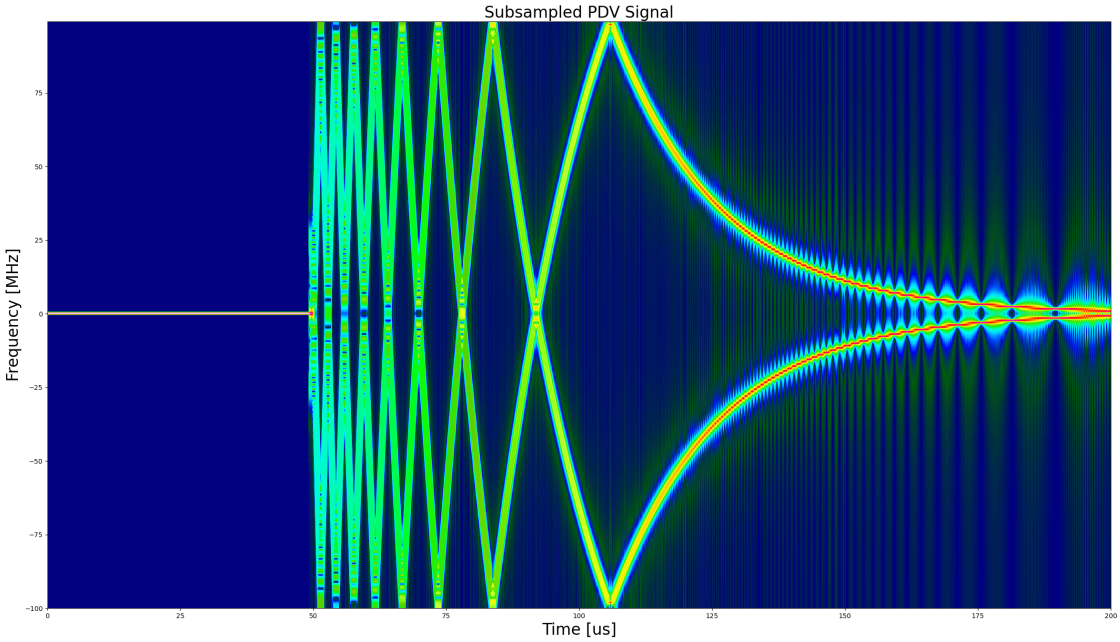

Fig. 6. Undersampled boiler-plate PDV signal prior to RF downconversion. The signal displayed in Fig. 5 is aliased into a 100 MHz Nyquist range with no additional processing.

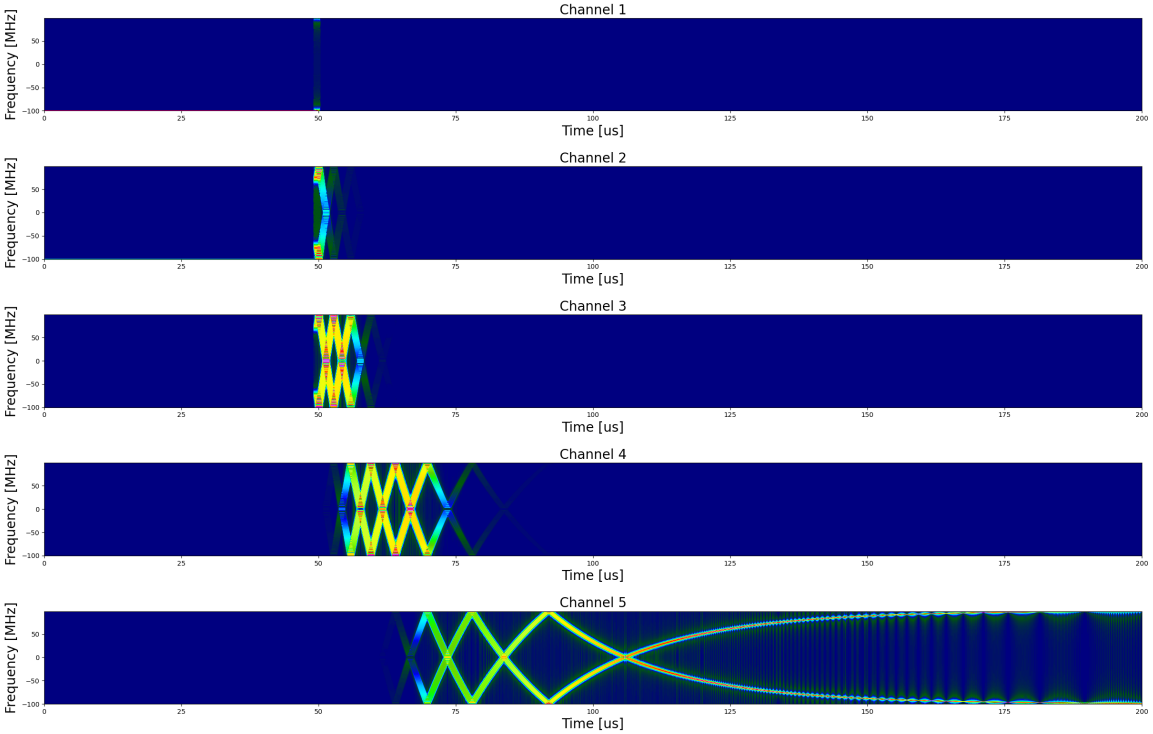

Fig. 7. Undersampled boiler-plate PDV signal with RF downconversion. The signal from Fig. 5 is now divided and downshifted according to frequency and aliased into 5 different 100 MHz channels. Note the behavior and appearance of the signal across multiple channels as the boiler-plate curve increases in frequency. Also worth noting is the absence of output on Channel 1 due to the signal's near-instantaneous initial rise time (jump-off).

Fig. 8. Red Pitaya [6]. SMA I/O headers for RF data acquisition can be noted on the front edge of the board.

multiple can be used in parallel while still taking up very little volume [6].

B. System Parameters and RF Design

With the Red Pitaya SDR122-16 digitizer, the bandwidth and frequency conversion parameters can now be set. Recalling the specifications of the digitizer and using the 550 MHz input bandwidth as a guideline, the channel division bandwidth for the frequency conversion can be set to 500 MHz for simplicity. With the inclusion of negative frequency content as described previously, the local oscillator spacing can also be set. This becomes twice the channel width, or 1000 MHz in this case. Therefore, assuming ideal components, the number of channels is trivial to extract: a 4 GHz signal shift divided into 1000 MHz channels results in 4 mixer channels. The divided bands then become 0 – 1000 MHz, 1000 – 2000 MHz, 2000 – 3000 MHz, and 3000 – 4000 MHz. These 4 bands require the use of two Red Pitayas, as each SDR122-16 only includes two RF input channels.

Mini-Circuits components were chosen for most of the connectorized elements in the block diagram, as they are low-cost and typically have high availability from multiple retailers. Mixers such as Mini Circuits ZX05-83LH-S+ were selected, with some variation on exact part number depending on mixer band. Small resistive splitters such as Mini Circuits ZFRSC-4-842-S+ were used for the power division step, and amplifiers such as Mini Circuits ZX60-6013E-S+ were also procured [7]. A generalized block diagram of the RF downconversion system is displayed in Figure 9.

System performance of the benchtop setup was acceptable, but left room for improvement. One primary drawback was the decision to use resistive splitters over a different topology, as resistive splitters only offer about 6 dB of isolation between the output ports [7]. This resulted in spurious content showing up relatively unattenuated between output ports, reducing the effectiveness of the channel division.

C. Local Oscillator Considerations

This benchtop system requires a set of multiple, different local oscillator signals to feed the mixers. Keeping with the motivation for this investigation, the solution for generating the LOs must also be small, low power, and low complexity. Many possible solutions exist, but for brevity one simple example will be considered here. Finding a solution to generating the LOs without needing four separate oscillators or signal generators would be the most ideal. With this in mind, and looking carefully at the frequencies chosen when developing the design, it becomes apparent that they are all exact harmonics of the target signal bandwidth, 500 MHz. This relationship can be exploited to streamline the hardware used.

A class of passive RF components known as Comb Generators are useful for generating harmonic content from a single oscillator input. Nonlinear Transmission Line (NLTL) combs, as the name suggests, take advantage of transmission line nonlinearities to generate signal harmonics, including the fundamental [12]. A small NLTL comb generator from Marki Microwave was procured for use in generating the LOs for each channel [12], and is shown in Figure 10. Then, small band-pass filters were used to select individual LO ”pickets” from the comb generator output. Admittedly, this role could be filled by utilizing multiple signal generators, but to minimize complexity and number of benchtop tools required for testing, this approach was used.

V. Integrated System Design

The next step for continuing this design and investigation is implementing the RF downconversion hardware into a custom PCB and microstrip solution. A general overview of the design concept and some detailed design will be discussed here, but a full design is not included due to its continued development. Early component selection and hardware design of the custom solution was developed in parallel with evaluating the preliminary benchtop system. Connectorized components take up much more volume when compared to RF integrated circuits (ICs), and connecting several parts with cabling quickly begins to become unwieldy. Additionally, designing custom hardware gives the designer detailed control over certain parameters (splitter bandwidth and S parameters, for example).

As with the system requirements and preliminary design, component availability and application support are critical for the selection of integrated components to ensure practicality of rapid production. Thus, ICs with well-defined and annotated application schematics and evaluation circuits were preferred over alternatives.

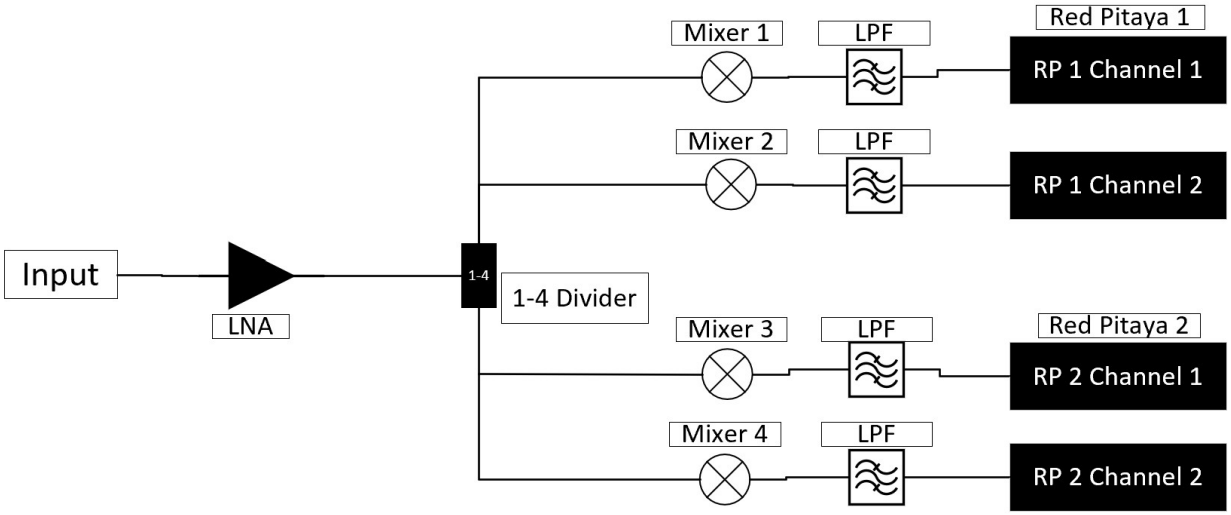

Fig. 9. RF conversion system block diagram. Signal is split between channels, and shifted into the input range of the Red Pitaya.

Fig. 10. Marki Microwave NLTL Comb Generator [12].

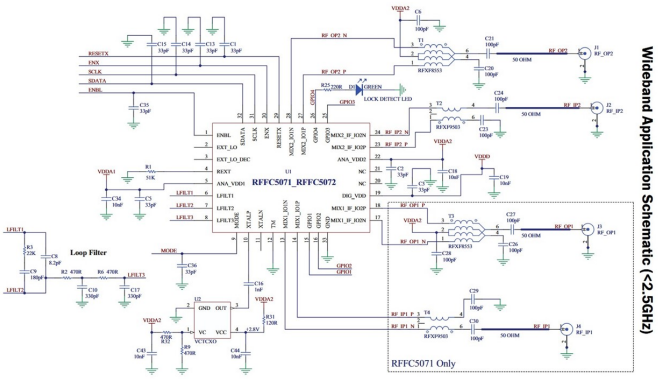

Fig. 11. Qorvo mixer application schematic [8].

A. Integrated Mixers

The mixer ICs selected for this design were Qorvo RFFC507x, which are chips containing mixers with integrated PLL VCOs [8]. There is a vast amount of documentation and support for these ICs including detailed application schematics for wideband frequency conversion, which is the exact application needed for this design. The Qorvo ICs use a proprietary serial protocol to communicate with control registers on the IC to set oscillator frequency, oscillator prescalar values, and current settings. The mixer IC bandwidth is configured via external RF front end baluns, which also convert 50 ohm input transmission lines to balanced input/output lines for the mixer RF and IF ports [8].

As the system design uses 4 mixer channels to create four outputs, the custom design will require 4 RFFC5072 ICs with supporting components. Each IC also supports grouping up to 4 of the control signals into a bus to communicate with a single serial port, which is ideal for this application as well [8]. Onboard control and generation of local oscillator signals is an incredibly useful feature, as it completely eliminates the issue of generating four LOs presented in the benchtop design, reducing hardware complexity significantly. The control lines can be connected to the Red Pitaya GPIO pins and easily controlled externally [6].

B. Power Divider Design

As detailed in the previous segment describing the benchtop design, the resistive dividers selected for splitting

the input signal amongst the four mixer channels have insufficient isolation between the output ports. This results in isolation between output ports (S23 and S32 for a 1-2 resistive divider) of about 6 dB [7]. This is a known characteristic of resistive dividers, and resulted in less-than-ideal suppression of spurious content showing up on the digitizer ports, as any reflections or generally unwanted signal content is not suppressed sufficiently between channels.

Because the finalized design is to be implemented as a custom PCB, there is freedom to also customize the RF divider in front of the mixers. That is, there is room within the SWaP constraints of the system design to implement an optimized power divider in microstrip within the PCB in order to better control the isolation between output channels. One divider topology that offers increased output isolation is the Wilkinson divider, which uses chip resistors in microstrip to isolate each ¼-wavelength segment from the next. Thus, a microstrip Wilkinson power divider topology was selected for design and included in the custom solution. However, basic single-stage Wilkinson dividers typically only support a narrow bandwidth, so a multi-section design will need to be implemented to widen the bandwidth to the full 4 GHz. Additionally, multiple 1 to 2 dividers will be cascaded to create the 1 to 4 channel split required to support this system design. A 1 to 2 splitter will thus be the primary focus of this design, as they form the building blocks of the 1 to 4.

Multistage Wilkinson dividers use the design equations of Chebyshev-polynomial ¼-wave impedance transformers to determine segment line impedance and isolation resistor values for each of n stages, or sections, of the divider. This expands the supported bandwidth of the return loss and isolation S parameters (S11, S23, and S32 for a 1-2 divider) [9]. The full design equations will not be derived here, but an overview will be included. Each stage of the divider must be ¼-wave in electrical length, which is determined based on substrate parameters.

Due to the nature of the PDV input signal, the fractional bandwidth of the divider must be as close to the theoretical maximum of 200% as possible. The center of the input band is 2 GHz and the maximum input frequency is 4 GHz. Input and output transmission line impedances are set to 50 ohm, following the requirements set forth in the application schematic shown in the previous section. The number of stages for the ¼-wave sections was set to $n = 3$, to maximize the useable bandwidth while conserving as much board space as possible.

Design Table 5.2 from [9] was used to select normalized impedance numbers, using $\Gamma_m = 0.05$ as minimized ripple is ideal for consistency across the divider passband. Using $N = 3$ and $\Gamma_m = 0.05$, with impedance ratio of $100\Omega/50\Omega = 2$, the normalized impedances are given as

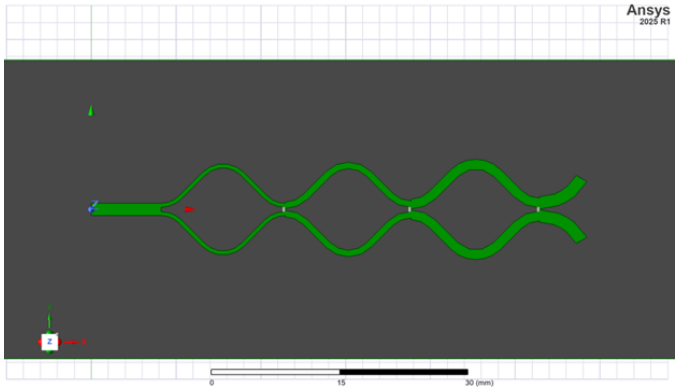

Fig. 12. 1 to 2 multisection Wilkinson divider layout, $n = 3$.

$z1 = 1.1475$, $z2 = 1.4142$, and $z3 = 1.7429$.

which when multiplied with $Z0 = 50\Omega$ gives the segment impedances as:

$Z1 = 57.34\Omega$, $Z2 = 70.71\Omega$, and $Z3 = 87.15\Omega$.

Using the normalized impedance values for the transmission line segments, the isolation resistor values can be computed using the expanded fraction found in [10]. First, the impedances need to be converted to admittances for convenience:

$y1 = 0.8715$, $y2 = 0.7071$, and $y3 = 0.4057$

Substituting these values into the expanded fraction for $n = 3$, the resistance values are then computed to be approximately

$r1 = 389\Omega$, $r2 = 130\Omega$, and $r3 = 92\Omega$.

The final divider design uses curved ¼-wave transmission line sections to reduce the overall length while retaining distance between each trace segment to prevent unwanted trace-to-trace coupling. 50 ohm lines are used in between the cascaded sections and on the input and output to ensure impedance match and to minimize internal reflections. To conserve space, the cascaded dividers in the 1 to 4 configuration were mirrored 180 degrees to conserve space on the board layout. Figures 12-15 show the simulated S-parameters and microstrip layouts of the individual 1 to 2 divider and cascaded 1 to 4 divider.

C. PCB Integration

The RF PCB was designed as a four layer board, with the RF components and microstrip populating the top layer. The Wilkinson divider was designed and simulated for a substrate of 30 mil FR4, with $\epsilon_r = 4.4$. This defines the top two layers of the PCB, as the second layer must be a solid

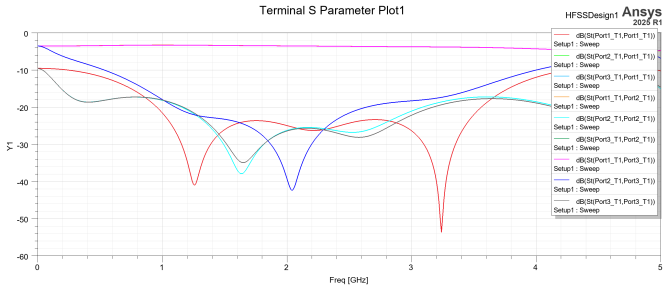

Fig. 13. 1 to 2 multisection Wilkinson divider S-parameters, $n = 3$. Sufficient isolation (10 dB or more) is observed for majority of the 4 GHz band.

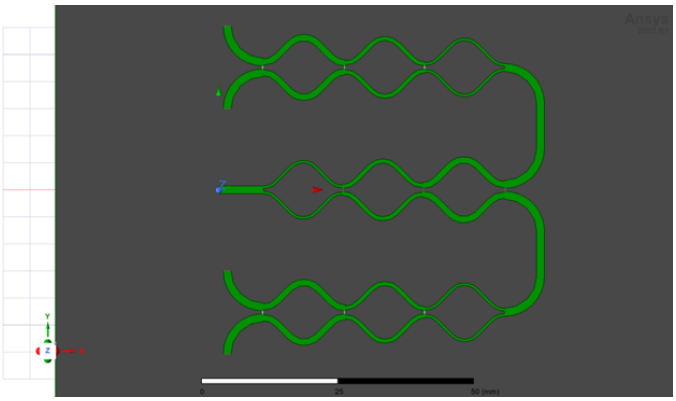

Fig. 14. Cascaded 1 to 4 multisection Wilkinson divider layout, $n = 3$.

ground plane to support the microstrip divider. The mixer ICs, supporting components, and connectors also are relegated to the top plane to facilitate the connection of the divider output transmission lines to the mixer ports. SMA connectors were preliminarily chosen for the RF connections for ease of use. The bottom two planes are left for power planes, additional ground planes, and signal traces.

VI. Conclusions

This investigation presented a novel design for an RF digitization system to support a PDV flyer-plate experiment. A benchtop evaluation design as well as a possible design for an integrated PCB were discussed, along with modeling and evaluation of theoretical system behavior. At the time of writing this report, the benchtop system is in testing with live PDV experiments and has produced positive results. The integrated design discussed above has yet to be fabricated, but some components are in the process of being evaluated.

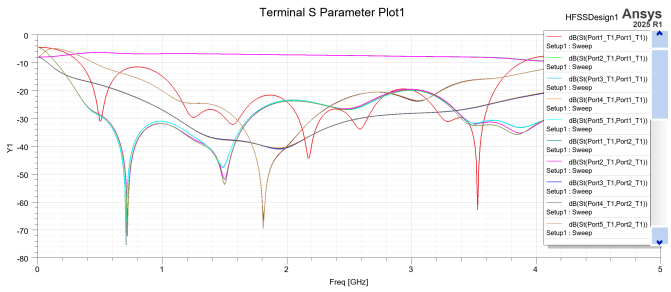

Fig. 15. Cascaded 1 to 4 multisection Wilkinson divider S-parameters, $n = 3$. Sufficient isolation still observed.

A. Discussion

Where the sub-Nyquist digitization system proves to be most useful is determining difference or variation between repeated experiments. The aliased and wrapped signal provides some understanding of the behavior of the experiment, especially when combined with information gained by dividing the signal band into multiple channels, but it is most useful when applied as a point of comparison in environments where full-scale PDV measurement equipment is not feasible. An experiment can be completed in a laboratory setting and the data acquired with a normal laboratory-grade oscilloscope and digitizer, and this "ground truth" experiment can be manipulated with a similar computer model to predict what the aliased and folded signal will become. Then, the same experiment is repeated in a constrained environment using the system described in this report, and the results are compared to detect the presence or absence of deviation between the two experiments.

B. Future Works

Further work could be done to investigate the feasibility of graphically "unwrapping" the aliased output signal, either by detecting zero-crossings in the output data or by hand. The primary challenge with this, as detailed previously, is identifying the end of the jump-off rising edge, and determining where the final range of the signal is. Extracting the shape of the resultant curve may not be difficult, but the location of the curve within the vertical axis may be impossible to determine. The feasibility of extracting the output plot also varies with the experiment itself, as accelerations and curve shapes can vary significantly from experiment to experiment. A slower, lower acceleration may have less of a jump-off, and may thus be easier to unravel post-aliasing, for example.

References

[1] P. D. Sargis, N. E. Molau, and D. Sweider, "Photonic Doppler Velocimetry," Engineering Research, Development and Technology, pp. 4-77-4–79. Accessed: 2025. [Online]. Available: https://www.osti.gov/servlets/purl/15013112#page=181

[2] D. H. Dolan, "Extreme measurements with Photonic Doppler Velocimetry (PDV)." 2020

[3] L. Sun et al., "Optimizing cure temperature of polyimide flyer for exploding foil initiator applications," Journal of Applied Polymer Science, vol. 139, no. 44, Aug. 2022.

[4] R. Baraniuk, "10.5: Aliasing phenomena," Engineering LibreTexts, https://eng.libretexts.org/Bookshelves/Electrical_Engineering/Signal_Processing_and_Modeling/Signals_and_Systems_(Baraniuk_et_al.)/10\%3A_Sampling_and_Reconstruction/10.05\%3A_Aliasing_Phenomena(accessedOct.19,2025).

[5] D. Herres, “The difference between signal under-sampling, aliasing, and folding” Test Measurement Tips, https://www.testandmeasurementtips.com/the-difference-between-signal-under-sampling-aliasing-and-folding-faq/ (accessed Oct. 19, 2025).
[6] “SDRlab 122-16 standard kit - red pitaya,” Red Pitaya, https://redpitaya.com/product/sdrlab-122-16-standard-kit/ (accessed Oct. 20, 2025).
[7] “Products,” Mini Circuits, https://www.minicircuits.com/ (accessed Oct. 19, 2025).
[8] “RFFC5071/5072 Datasheet.” Qorvo, Greensboro, NC, 2014
[9] D. M. Pozar, Microwave Engineering, 4th ed. Hoboken, NJ: Wiley, 2012.
[10] J. Wei, T. Ling, and L. Sun, “An ultra-wideband Compact 1 to 8 wilkinson power divider,” 2023 International Conference on Microwave and Millimeter Wave Technology (ICMMT), pp. 1–3, May 2023. doi:10.1109/icmmt58241.2023.10276729
[11] C. E. Shannon, “Communication in the presence of noise,” Proceedings of the IRE, vol. 37, no. 1, pp. 10–21, Jan. 1949. doi:10.1109/jrproc.1949.232969
[12] “NLTL-6273S_GaAs MMIC non-linear transmission line,” NLTL-6273S, https://markimicrowave.com/products/connectorized/nltl-comb-generators/nltl-6273s/datasheet/ (accessed Oct. 20, 2025).